





Drosophila carboxypeptidase D (SILVER) is a key enzyme in neuropeptide processing required to maintain locomotor activity levels and survival rate

Dennis Pauls¹  | Yasin Hamarat^{1,2}  | Luisa Trufasu¹ | Tim M. Schendzielorz¹ | Gertrud Gramlich¹ | Jörg Kahnt³ | Jens T. Vanselow⁴  | Andreas Schlosser⁴ | Christian Wegener¹ 

¹Neurobiology and Genetics, Theodor-Boveri-Institute, Biocenter, University of Würzburg, Würzburg, Germany

²'Santaka' Valley I Health Telematics Science Institute, Kaunas University of Technology, Kaunas, Lithuania

³Max-Planck-Institute of Terrestrial Microbiology, Marburg, Germany

⁴Rudolf Virchow Center for Experimental Biomedicine, University of Würzburg, Würzburg, Germany

Correspondence

Christian Wegener, Neurobiology and Genetics, Theodor-Boveri-Institute, Biocenter, University of Würzburg, Am Hubland, D-97074 Würzburg, Germany. Email: christian.wegener@biozentrum.uni-wuerzburg.de

Funding information

University of Würzburg

The peer review history for this article is available at <https://publons.com/publon/10.1111/EJN.14516>

Abstract

Neuropeptides are processed from larger preproteins by a dedicated set of enzymes. The molecular and biochemical mechanisms underlying preproprotein processing and the functional importance of processing enzymes are well-characterised in mammals, but little studied outside this group. In contrast to mammals, *Drosophila melanogaster* lacks a gene for carboxypeptidase E (CPE), a key enzyme for mammalian peptide processing. By combining peptidomics and neurogenetics, we addressed the role of carboxypeptidase D (dCPD) in global neuropeptide processing and selected peptide-regulated behaviours in *Drosophila*. We found that a deficiency in dCPD results in C-terminally extended peptides across the peptidome, suggesting that dCPD took over CPE function in the fruit fly. dCPD is widely expressed throughout the nervous system, including peptidergic neurons in the mushroom body and neuroendocrine cells expressing adipokinetic hormone. Conditional hypomorphic mutation in the dCPD-encoding gene *silver* in the larva causes lethality, and leads to deficits in starvation-induced hyperactivity and appetitive gustatory preference, as well as to reduced viability and activity levels in adults. A phylogenomic analysis suggests that loss of CPE is not common to insects, but only occurred in Hymenoptera and Diptera. Our results show that dCPD is a key enzyme for neuropeptide processing and peptide-regulated behaviour in *Drosophila*. dCPD thus appears as a suitable target to genetically shut down total neuropeptide production in peptidergic neurons. The persistent occurrence of CPD in insect genomes may point to important further CPD functions beyond neuropeptide processing which cannot be fulfilled by CPE.

KEYWORDS

direct mass spectrometric profiling, fruit fly behaviour, M14 carboxypeptidases, peptidomics, proprotein processing

Edited by Giovanni Galizia.

This is an open access article under the terms of the Creative Commons Attribution-NonCommercial License, which permits use, distribution and reproduction in any medium, provided the original work is properly cited and is not used for commercial purposes.

© 2019 The Authors. *European Journal of Neuroscience* published by Federation of European Neuroscience Societies and John Wiley & Sons Ltd.

1 | INTRODUCTION

Neuropeptides and peptide hormones are synthesised as parts of larger precursors (preproteins) from which they are sequentially processed into their bioactive form by sequential action of proprotein convertases (PCs), carboxypeptidases (CPs) and amidating enzymes (Fricker, 2005; Zhou, Webb, Zhu, & Steiner, 1999). In mammals, proprotein processing is well-characterised on the molecular and biochemical level, and is implicated in a variety of physiological and pathological processes including obesity and growth defects (Seidah & Prat, 2012; Taylor, Van de Ven, & Creemers, 2003). In contrast, the mechanisms and functions of proprotein processing are little studied in lower vertebrate taxa and invertebrates.

For insects, proprotein processing is best understood for *Drosophila melanogaster* (reviewed by Pauls et al., 2014). In the fruit fly, the first processing step is catalysed by the proprotein convertase dPC2 encoded by the gene *amontillado* (*amon*; Rayburn et al., 2003; Siekhaus & Fuller, 1999; Wegener, Herbert, Kahnt, Bender, & Rhea, 2011). A deficiency in dPC2 results in reduced or absent levels of neuro- and enteroendocrine peptides (Reiher et al., 2011; Rhea, Wegener, & Bender, 2010; Wegener et al., 2011), developmental defects and impaired behaviour including hatching and ecdysis (Rayburn, Rhea, Jocoy, & Bender, 2009; Rayburn et al., 2003; Siekhaus & Fuller, 1999) and larval locomotion (Wegener et al., 2011) as well as carbohydrate metabolism (Rhea et al., 2010).

As a typical PC, dPC2 cuts C-terminal of canonic mono- or dibasic amino acid (typically R, KR or RR) cleavage sites, resulting in peptides which are C-terminally extended by basic amino acids. In mammals, these basic C-terminal extensions are pruned by N/E metallo-carboxypeptidase E (CPE, EC 3.4.17.10; Che & Fricker, 2002; Che et al., 2001; Fricker & Snyder, 1982), which initially was thought to be the only carboxypeptidase involved in neuropeptide processing (Fricker, 2013a). However, a further member of the M14B subfamily of metallo-carboxypeptidases, carboxypeptidase D (CPD, EC 3.4.17.22), was later found to be able to partially compensate for a loss of CPE action (Song & Fricker, 1995). CPDs are unusual in that they are large proteins (~180 kDa) that contain three CP domains. Only the first two domains are enzymatically active, while the third domain is inactive (Fricker, 2013a; Garcia-Pardo et al., 2017). In contrast, CPEs and other M14B CPs like the membrane-bound CPM (EC 3.4.17.12) are smaller (52–56 kDa) and contain only one CP domain (Fricker, 2013b; Zhang & Skidgel, 2013).

Curiously, unlike vertebrates and most other invertebrates, *Drosophila* lacks a CPE gene and only possesses a CPD-encoding gene named *silver* (Settle, Green, & Burtis, 1995). The two active domains of dCPD differ in their pH optima and substrate preferences (Sidyelyeva, Baker, & Fricker, 2006; Sidyelyeva & Fricker, 2002; Sidyelyeva et al.,

2010). While null mutations in *svr* are lethal (Bourbon et al., 2002), dCPD transgenes containing either active domain 1 or domain 2 can rescue behavioural and developmental deficits of *svr* mutant flies to varying degrees (Sidyelyeva et al., 2010). Hypomorphic mutants have defects in cuticle melanisation and tanning, wing morphogenesis, biogenic amine metabolism, light response (Lindsley & Grell, 1968; Wright, 1987) and memory formation (Lu et al., 2016; Sidyelyeva et al., 2010), and show increased ethanol and cold sensitivity (Sidyelyeva et al., 2010).

The general requirement of CPs in neuropeptide and peptide hormone processing and the lack of a CPE gene in the *Drosophila* genome imply that dCPD is functionally important for the production of bioactive peptides in the fruit fly. This reasoning is supported by a prominent expression of *svr* in the central nervous system (CNS) and endocrine tissues such as the midgut (Chintapalli, Wang, & Dow, 2007), as well as by the direct transactivation of *svr* by the basic helix–loop–helix transcription factor DIMMED which confers a neuroendocrine peptidergic phenotype (Hadžić et al., 2015). Ectopic expression of *svr* transgenes in the neurohemal organ of the brain (corpora cardiaca) also affects processing of adipokinetic hormone (AKH; Sidyelyeva et al., 2010). Yet, direct and comprehensive biochemical evidence for a role of dCPD or any other CPD in neuropeptide processing is lacking.

Here, we used a combined neurogenetic–peptidomic approach to test the requirement of dCPD for neuropeptide processing, locomotor behaviour and life span. A phylogenomic search for CPD and CPE genes throughout the insects suggests that CPE has been independently lost in a few holometabolous insect taxa, while all analysed insect species likely possess CPD. Taken together, our results suggest that insect CPDs can fully compensate for a loss of CPE.

2 | MATERIALS AND METHODS

2.1 | *Drosophila melanogaster* strains

The *svr* null mutant $y^1w^*P\{w^{+mWhs}=GawB\}svr^{PG33}/FM7h$ (Bourbon et al., 2002) was a kind gift of Galina Sidyelyeva and Lloyd Fricker. w^{1118} controls, $10xUAS-IVS-myr::GFP$ and $UAS-Stinger$ were obtained from Bloomington Stock Center. Flies were kept on standard food at either 18°C or 25°C and an LD12:12 light cycle and a relative humidity of 60%.

2.2 | Generation of *hs-svr* flies

To rescue the lethal *svr*^{PG33} mutant phenotype, we generated flies carrying a *hs-svr*^{1A-2-3-t2} genomic insert. The pUAST-*svr* (1A-2-3-t2) plasmid (Sidyelyeva et al., 2010, kind gift of Galina Sidyelyeva and Lloyd Fricker) was digested using *EcoRI* and *XbaI*, resulting in two fragments consisting of

the 5'-2,174 bp and the 3'-2,351 bp part of the *svr* (1A-2-3-t2) construct. Then, the pCaSpeR-hs vector (Thummel & Pirrotta, 1991) was digested using *EcoRI* and *XbaI*, and the 3'-2,351 bp part was inserted. After ligation, the resulting plasmid was digested with *EcoRI*, and the 5'-2,174-bp fragment was inserted and ligated. The correct orientation of the fragments and sequence was confirmed by sequencing, and the resulting *hs-svr* construct (1A-2-3-t2) was introduced into the germline of w^{1118} flies by BestGene using standard P-element transformation. Several independent transformant lines were obtained which were used to generate w^{1118} ; $hs-svr^{1A-2-3-t2}$ and $y^1 w^* P\{w^{+mWhs}=GawB\}svr^{PG33}/FM7h$; $hs-svr^{1A-2-3-t2}$ lines.

2.3 | Heat-shock rescue

Eggs of $y^1 w^* P\{w^{+mWhs}=GawB\}svr^{PG33}/FM7h$; $hs-svr^{1A-2-3-t2}$ flies were collected every morning, kept at room temperature and heat-shocked daily for 30 min at 37°C in a water bath. Larvae for the behavioural assays were obtained by heat shocking for 4 days, followed by two days at 18°C to minimise background expression of *hs-svr*. Homozygous mutant larvae were identified by the light mouthparts and unpigmented denticle bands due to the y^1 allele, while larvae carrying FM7h showed stronger pigmentation due to the y^{31} allele of FM7h (Brehme, 1941). To obtain adults, heat shocking was continued until eclosion. After eclosion, flies were kept at 18°C for the times indicated. Then, male flies were anaesthetised on ice and nervous tissue was dissected and processed as described below. FM7h controls were distinguished from svr^{PG33} mutants by the presence of bar (*B*) and orange-coloured eyes.

2.4 | RT-PCR

To test for background expression of *hs-svr*, total RNA was extracted from heads of five adult males per genotype using the Quick-RNA MicroPrep Kit (Zymo Research) according to manufacturer's instructions. Heads were cut off, collected in a microtube containing 300 µl RNA lysis buffer on ice and homogenised with a plastic pestle. Total RNA was eluted in 8 µl RNase-free water. For cDNA synthesis, the QuantiTect Reverse Transcription Kit from Qiagen was used. All steps were performed following the manufacturer's protocol. Genomic DNA was removed by adding 1 µl of gDNA wipeout buffer to 6 µl of the eluted RNA. Following incubation at 42°C for 2 min, the samples were placed for 2 min at 4°C and 3 µl of a mastermix composed of 8 µl RT Buffer, 2 µl RT Primer Mix and 2 µl reverse transcriptase was added. Reverse transcription was performed for 30 min at 42°C, followed by 3 min at 95°C and 2 min at 4°C. Finally, 40 µl of water was added and cDNA samples were stored at -20°C.

cDNA was PCR-amplified using a JumpStart REDTaq ReadyMix (Sigma-Aldrich) and *svr*-, *GawB*- and *Gaw-svr*-specific primers (see Table S1). α -tubulin was used as internal control. The PCR programme consisted of 5 min at 95°C, followed by 30 cycles of 30 s at 95°C, 30 s at 60°C and 60 s at 72°C, and followed by a final extension for 5 min at 72°C.

2.5 | Direct peptide profiling via MALDI-TOF mass spectrometry

Direct peptide profiling was carried out according to our standard protocol (Wegener, Neupert, & Predel, 2010). In brief, the brain and ventral ganglion (VG) of 14-day-old adult male flies were dissected in HL3.1 saline (Feng, Ueda, & Wu, 2004). Using microscissors, the brain was further divided into optic lobes or central brain. Tissues were then transferred by pulled glass capillaries to a stainless steel MALDI target, remaining saline was removed and the tissues were let to dry. In case of excess salt deposits, a small droplet of ice-cold water was added to the dried tissues and removed after about 1 s to desalt the sample.

Then, 200 nl matrix (saturated solutions of recrystallised *a*-cyano-4-hydroxycinnamic acid [CHCA]; Sigma) in 30% MeOH: 30% EtOH and 40% water (v:v:v) was added per tissue and let to dry. MALDI-TOF mass spectra were acquired in positive ion mode on an Applied Biosystems 4800 Plus MALDI-TOF/TOF mass spectrometer (Applied Biosystems/MDS Sciex). Samples were analysed in positive reflector mode within a mass window of 850–3,000 Da. Some mass peaks were additionally fragmented in MS/MS mode using PSD. Laser power was adjusted manually to provide optimal signal-to-noise ratio. Raw data were analysed using Data Explorer 4.10 software (Applied Biosystems/MDS Sciex).

2.6 | Sample preparation for NanoLC-ESI-MS/MS

After eclosion, flies were kept for 5 days without heat shock. Then, brains and ventral nerve cords of males were dissected in HL3.1 saline on ice and transferred by a needle to a frozen microtube in a laptop cooler. Per sample, 30 brains plus ventral nerve cords were pooled and stored at -80°C until extraction. For extraction, 50 µl of a methanol, water and trifluoroacetic acid mixture (90/9/1 v/v/v) was added to the frozen tubes, followed by 3 min in an ice-cold ultrasonic bath and 30 min of incubation on ice. Afterwards, the samples were centrifuged at 15,000 g (Hettich Mikro), and the supernatant was transferred to a new microtube and vacuum-dried (Uniequip Univapo 100H).

The extracts were prepurified on self-made StageTips (Rappsilber, Mann, & Ishihama, 2007) using 3M Empore C18 material (ChromTech Inc.) and 200-µl pipet tips. The columns were activated with 50 µl of 100% acetonitrile and

equilibrated with 50 μ l of 10 mM HCl. The extracted samples were dissolved in 30 μ l of 10 mM HCl, sonicated in an ultrasound bath and applied onto the equilibrated StageTips. After washing with 50 μ l 10 mM HCl, peptides were eluted with 30% acetonitrile and dried in a vacuum concentrator (SpeedVac, Eppendorf). Low-binding plastic was used throughout.

2.7 | NanoLC-MS/MS analysis

Peptides were dissolved in 2% acetonitrile and 0.1% formic acid. NanoLC-MS/MS analyses were performed on an Orbitrap Fusion (Thermo Scientific) equipped with a PicoView Ion Source (New Objective) and coupled to an EASY-nLC 1000 (Thermo Scientific). Peptides were loaded on capillary columns (PicoFrit, 30 cm \times 150 μ m ID, New Objective) self-packed with ReproSil-Pur 120 C18-AQ, 1.9 μ m (Dr. Maisch) and separated with a 30-min linear gradient from 3% to 40% acetonitrile and 0.1% formic acid and a flow rate of 500 nl/min.

Both MS and MS/MS scans were acquired in the Orbitrap analyzer with a resolution of 60,000 for MS scans and 15,000 for MS/MS scans. A mixed ETD/HCD method was used. HCD fragmentation was applied with 35% normalised collision energy. For ETD, calibrated charge-dependent ETD parameter was applied. A Top Speed data-dependent MS/MS method with a fixed cycle time of 3 s was used. Dynamic exclusion was applied with a repeat count of 1 and an exclusion duration of 10 s; singly charged precursors were excluded from selection. Minimum signal threshold for precursor selection was set to 50,000. Predictive AGC was used with AGC, a target value of 2e5 for MS scans and 5e4 for MS/MS scans. EASY-IC was used for internal calibration.

In total, three (controls) and two (mutants) biological samples were measured in technical duplicates. All chemicals used were of HPLC grade; low-binding plastic was used throughout.

2.8 | Data analysis

Data analysis was performed with PEAKS Studio 8.5 (Bioinformatics Solutions Inc.; Zhang et al., 2012). Parent mass tolerance was set to 8 ppm, and fragment mass tolerance to 0.02 Da. Pyro-Glu (N-term Q), oxidation (Met), carbamidomethylation (Cys) and amidation (C-term) were allowed as variable modification. A maximum number of five modifications per peptide were allowed. Searches were performed against a custom neuropeptide database that contained all known *Drosophila* and suggested pre-peptides, processing enzymes and neuropeptide receptors. Results were filtered to 1% PSM-FDR. To calculate the processing index (PI), we first calculated the mean ratio R of the peak area (PA) between the fully processed

and unprocessed form ($R = PA_{\text{fully processed}}/PA_{\text{C-terminally extended}}$) for the mutant and control samples, respectively. These ratios were then used to calculate the PI for each peptide ($PI = R_{\text{svr}^{PG33} \text{ mutant}}/R_{\text{FM7h control}}$) which corrects for possible differences in the ionisation probabilities between processed and unprocessed peptides. In case a peptide was only detectable in its unprocessed form in mutants leading to a division by 0, the PI was set to 10^{-10} . Likewise, if a peptide was only detected in its processed form in the mutant but not the control, the PI was set to 2.

2.9 | Immunostainings

svr^{PG33}/FM7h flies were crossed with *w*^{*}, 10 \times UAS-IVS-myrGFP or *w*^{*}; UAS-Stinger. L3 larval CNS of the F1 progeny 2 days after last heat shock was dissected in HL3.1 saline (Feng et al., 2004) and fixed for 2 hr in 4% paraformaldehyde in 0.1 M PBS at room temperature. Then, the CNS was washed in 0.1 M PBS with 0.3% Triton X (PBT) and incubated in PBT + 5% normal goat serum for 1 hr at room temperature. Afterwards, primary antibodies (anti-GFP rabbit polyclonal [1:1,000; Invitrogen] and anti-brp [nc82] mouse monoclonal [mAb; 1:100]) in PBT + 5% NGS were added overnight at 4°C on a shaker. Preparations were then washed 5 \times for at least 1 hr in 1 \times PBS at room temperature. Fluorophore-coupled secondary antisera (goat anti-rabbit Alexa 488 and goat anti-mouse DyLight 649; Dianova GmbH), diluted 1:1,000 in PBT + 5% NGS, were added and preparations were incubated overnight at 4°C on a shaker. Next, preparations were washed as above, followed by a final wash in 0.1 PBS and mounting in 80% glycerol in 0.1 M PBS. The preparations were analysed with a Leica TCS SPE confocal microscope (Leica SPE, Leica Microsystems), using ACS APO 20 \times /0.60 and ACS APO 40 \times /1.15 objectives. Images were processed with Fiji (Schindelin et al., 2012) and Adobe Photoshop CS6 (Adobe Systems; V.6.0.1).

2.10 | Locomotor activity recording

Four- to seven-day-old flies were recorded individually with the *Drosophila* Activity Monitoring (DAM; TriKinetics) system. To record normal rhythmic behaviour, flies were kept in glass tubes with 2% agarose and 4% sugar on one side under standard 12:12 light:dark conditions with light intensities around 100 lux at 20°C and 60% humidity. Fly activity was defined by the number of infrared light beam crosses per minute or per day. Under starved conditions, flies were kept on 2% agarose to avoid dehydration.

2.11 | Survival

To test flies for changes in life span, groups of ten flies were kept under normal ad libitum standard food conditions at

25°C and 60% humidity and dead flies were counted at the end of each day. Flies were transferred onto fresh food every 3–4 days to circumvent influences due to changes in food quality.

2.12 | Larval preference tests

To test larvae for innate odour and taste preference, the FIM (FTIR-based Imaging Method) tracking system (Risse et al., 2013) was used to monitor individual larvae over time. Recordings were made by a monochrome industrial camera (DMK27BUP031) with a Pentax C2514-M objective in combination with a Schneider infrared pass filter, and the IC capture software (www.imagingsource.com). Larval position in relation to the odour or taste stimulus was determined every second. To test larvae for innate odour responses, a thin layer of 1.5% agarose was placed on an acryl plate which was illuminated with infrared light. An odour container (10 µl amyl-acetate) was placed on one side of the agarose layer. A group of five larvae was placed in the neutral midzone of the agarose layer, and larvae were recorded for 5 min. To monitor larval responses to fructose or high salt, larvae were placed on a 1.5% agarose layer which contained either 2 M fructose or 1.5% sodium chloride on one side.

Preference indices (PIs) were calculated by subtracting the number of larvae on the stimulus side (ST) from the number of larvae on the no-stimulus side (NO), divided by the total number of larvae: $PI = (\#ST - \#NO)/\#TOTAL$. Negative PI values indicate avoidance behaviour, while positive PI values indicate approach behaviour.

2.13 | Phylogenomic analysis

A genome-based tblastn search on the NCBI and i5k workspace@NAL website was performed, using the protein sequences for *Drosophila* CPD and *Caenorhabditis elegans* CPE as a query. The search was then repeated with identified putative insect CPE sequences. Incomplete hits were removed, resulting in a list of 313 CPE/D/M-like sequences that were analysed using MEGA X (Kumar, Stecher, Li, Knyaz, & Tamura, 2018). First, sequences were aligned using the Muscle algorithm, and then a maximum-likelihood tree employing the JTT matrix-based amino acid substitution model (Jones, Taylor, & Thornton, 1992) with all sites was calculated with a bootstrap value of 500.

2.14 | Statistical analysis

Data were tested for normal distribution using a Shapiro–Wilk test. For the comparison of genotypes, an unpaired two-sided *t* test (pairwise.t.test) was used for normally distributed data and an unpaired Wilcoxon rank-sum test for nonparametrically distributed data. Statistical analyses were

done with RStudio, Version 1.0.136 (www.r-project.org). Significance levels between genotypes shown in the figure refer to raw *p*-values obtained in the statistical tests.

3 | RESULTS

3.1 | Characterisation of the transgenic heat-shock rescue lines

The *svr*^{PG33} allele was generated via a genomic P-element mediated *PGawB* insertion into the second exon of *svr* on the first (X) chromosome (Bourbon et al., 2002). The insertion inhibits expression of *svr* mRNA (Sidyelyeva et al., 2006) leading to embryonal and early larval lethality in hemizygous males and homozygous females. To rescue lethality, we generated transgenic flies carrying a *hs-svr*^{1A-2-3-t2} genomic insert, which under the control of a heat-shock (*hs*) promoter expressed a transgenic and endogenously expressed CPD form consisting of an inactive first and third CP domain, and an active second CP domain, a transmembrane domain and the tail-2 region (Sidyelyeva et al., 2010). To test the functionality of the newly generated *hs-svr* rescue lines, we crossed *yw*^{*}*svr*^{PG33}/FM7h virgins with males of two different FM7/Y; *hs-svr* lines and kept the flies at constant 18°C or under a heat-shock regime. We then scored the F1 adult males for the dominant FM7 marker *Bar* (*B*). At constant 18°C, only *B* males (FM7/Y; *hs-svr*/+) were present in both crosses (59/40 males, respectively), confirming the early lethality of the homozygous *svr*^{PG33} genotype. Under heat-shock regime, both *B* and normal-eyed males were found (36:33/37:13, respectively), indicating a ≥35% heat-shock rescue efficiency for *svr*^{PG33}/Y males. Thus, the newly generated *hs-svr* lines are functional and can be used to rescue lethal *svr* mutations.

While a *hs*-promoter is ideal to drive rescue gene expression in nonfeeding developmental stages (egg, pupa), it is prone to low background expression at normal temperatures (Steller & Pirrotta, 1985). Using RT-PCR with *svr*-specific primers (Figure S1a), we found *svr* expression in *w*¹¹¹⁸ control flies containing a functional *svr* gene, in heat-shock-rescued *svr*^{PG33}, *hs-svr* mutant flies, and in *svr*^{PG33}, *hs-svr* flies maintained at 18°C (Figure S1b). To distinguish whether the *svr* expression in *svr*^{PG33}, *hs-svr* flies at low temperature is due to background expression from the *hs* transgene or expression from the endogenous *svr*^{PG33} allele, we performed RT-PCR with a *GawB*/*svr*^{PG33} insert-specific primer set (Figure S1c). *GawB* expression was absent from *w*¹¹¹⁸ controls, but detectable in heat-shock-rescued *svr*^{PG33} mutant flies. Again, a weak band was found for *svr*^{PG33}, *hs-svr* flies maintained at 18°C. A primer set spanning the region from the 3' end of *GawB* to *svr* exon 5 did not result in a detectable product in all flies and conditions tested. This confirms previous findings that the *PG*³³ insertion disrupts expression

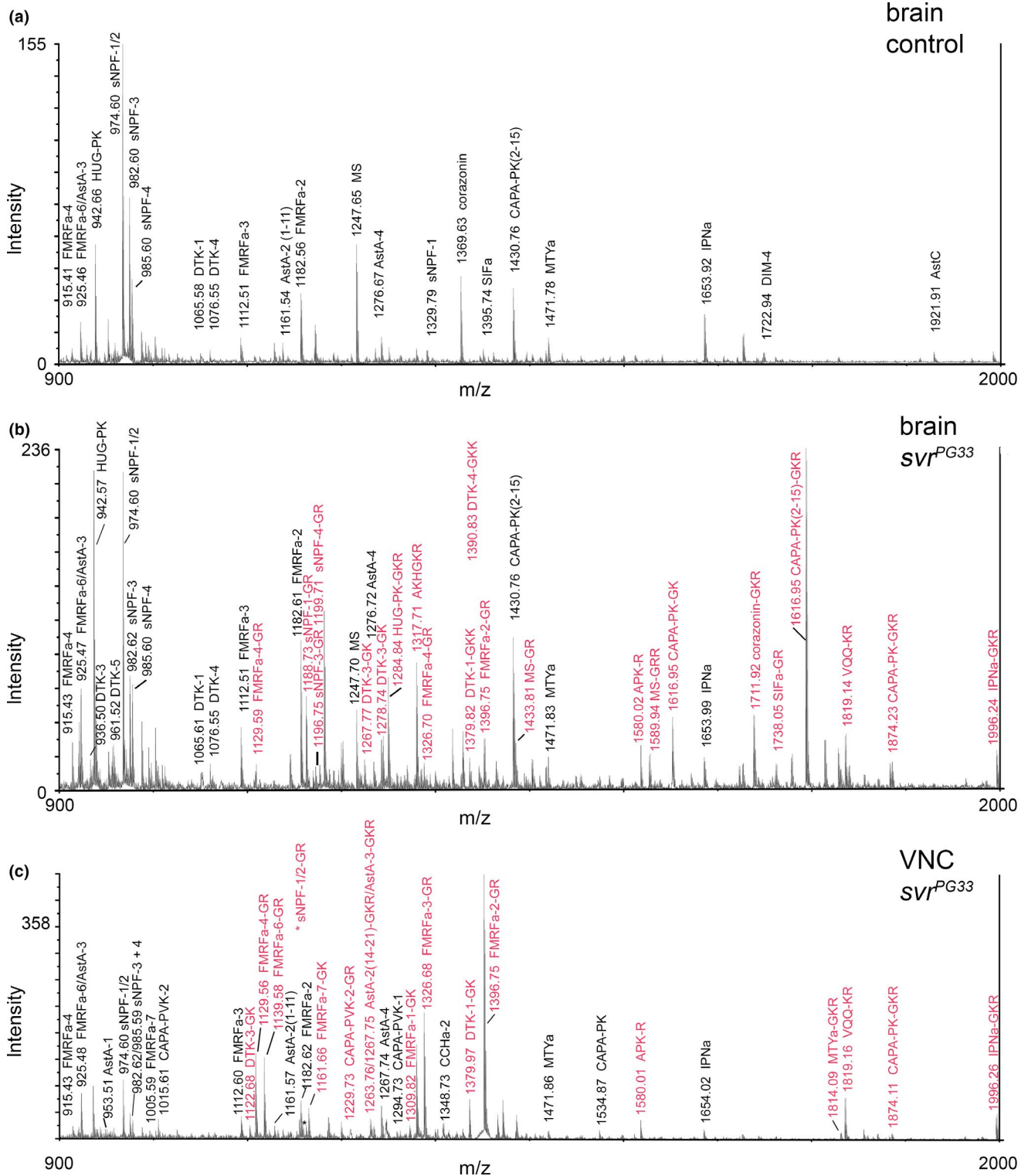


FIGURE 1 MALDI-TOF spectra from direct peptide profiling. (a) Example for central brain tissue of a *FM7h*; *hs-svr* control fly in the mass range of 900–2,000 Da. Note that all detected neuropeptides are fully processed, indicated by black letters. (b) Example for central brain tissue of a *svr^{PG33}*; *hs-svr* mutant fly. Note that the profile for fully processed neuropeptides (black letters) is very similar to that for controls in (a). Yet, in addition, peaks indicating C-terminally extended forms (red letters) are present. (c) Similar C-terminally extended forms are also visible in other tissues, here a ventral nerve cord of a *svr^{PG33}*; *hs-svr* mutant fly although a partly different neuropeptide complement is present. [Colour figure can be viewed at wileyonlinelibrary.com]

TABLE 1 Peptides detected by MALDI-TOF direct profiling (in green) and LC-MS (logarithm of the processing index PI is shown in colour-code). [Colour table can be viewed at wileyonlinelibrary.com]

peptide family	peptide	sequence fully processed	[M+H] ⁺	sequence C-terminally extended	[M+H] ⁺	sequence C-terminally extended	[M+H] ⁺	log ₁₀ PI
Allolactatin A	AsIA-1	VERVAFGLa	953.52	VERVAFGLGR	1167.63	VERVAFGLGRR	1323.73	-1.35
	AsIA-2	LPVYNFGLa	921.51	LPVYNFGLGK	1107.62	LPVYNFGLGKR	1263.72	-7.68
	AsIA-3	SRPYSFGLa	925.49	SRPYSFGLGK	1111.59	SRPYSFGLGKR	1267.69	-7.66
	AsIA-4	TRPQPFVGLa	1276.7	TRPQPFVGLGR	1490.79	TRPQPFVGLGRR	1646.89	-6.50
Allolactatin C	AsI-C	QVRYROYFNPISCF	1923.90	QVRYROYFNPISCFR	2080.00	QVRYROYFNPISCFRK	2208.10	-6.74
	CAPA-PVK-1	GANNMGLYAFPRV/a	1294.6	GANNMGLYAFPRVGR	1508.78	GANNMGLYAFPRVGRK	1664.88	-6.53
CAPA peptides	CAPA-PVK-2	ASGLVAFPRV/a	1015.6	ASGLVAFPRVGR	1229.71	ASGLVAFPRVGRK	1385.81	-7.22
	CAPA-PK	TFPSASSGLWFGPRL/a	1531.8	TFPSASSGLWFGPRLGK	1717.90	TFPSASSGLWFGPRLGKR	1874.00	-
CAPA-PK (2-15)	CAPA-PK	GFSASSGLWFGPRL/a	1430.75	GFSASSGLWFGPRLGK	1616.85	GFSASSGLWFGPRLGKR	1772.96	-
	CCAP	PFONAFGTCa	956.4	PFONAFGTGCGK	1170.50	PFONAFGTGCGKR	1298.59	-
Crustacean cardioactive peptide	CCHa2	GCOAYGHVCGGH/a	1348.53	GCOAYGHVCGGHGK	1534.60	GCOAYGHVCGGHGKR	1690.75	-
	Corazonin	pQTFQYSRGWtNa	1369.63	pQTFQYSRGWtNGK	1555.73	pQTFQYSRGWtNGKR	1711.83	-10.00
Diuretic hormone 31	DH31	TVDFGLARGYSGTQEAHRMGLAAANFAGGP/a	3149.27	TVDFGLARGYSGTQEAHRMGLAAANFAGGPGR	3363.68	TVDFGLARGYSGTQEAHRMGLAAANFAGGPGRK	3519.78	-8.38
	FMRFa-1	SVQDNFMHFa	1123.49	SVQDNFMHFGK	1309.60	SVQDNFMHFGKR	1465.70	-
FMRFa-like peptide	FMRFa-2	DPKQDFMRFa	1182.57	DPKQDFMRFGR	1396.68	DPKQDFMRFGRK	1552.78	-8.83
	FMRFa-3	TPAEDFMRFa	1112.52	TPAEDFMRFGR	1326.63	TPAEDFMRFGRK	1482.73	-7.99
	FMRFa-4	SDNFMRFa	915.41	SDNFMRFGR	1129.52	SDNFMRFGRK	1285.57	-7.67
	FMRFa-5	SPKQDFMRFa	1154.58	SPKQDFMRFGR	1368.68	SPKQDFMRFGRK	1524.73	-8.47
	FMRFa-6	PDNFMRFa	925.44	PDNFMRFGR	1139.54	PDNFMRFGRK	1295.59	-7.23
	FMRFa-7	SAPQDFVRSa	1005.51	SAPQDFVRSKGK	1191.61	SAPQDFVRSKGKR	1347.66	-7.86
	FMRFa-8	MDSNFRFa	1028.5	MDSNFRFGK	1214.60	MDSNFRFGKR	1370.65	-7.01
HUGN-pyrkinin	HUG - PK	942.58	SVPFKRL/a	1128.69	SVPFKRLGK	1284.79	-7.43	
Kinin	kinin	NSVVLGKKQRHSHWG/a	1741.96	NSVVLGKKQRHSHWGK	1928.06	NSVVLGKKQRHSHWGKR	2084.16	-1.40
	Mysuppressin	MIP-1	1091.52	AWQSLQSW/a	1277.63	AWQSLQSWGK	1433.73	-10.00
Mysuppressin	MIP-2	AWKSMNV/a	1091.54	AWKSMNVWGK	1277.65	AWKSMNVWGKR	1433.75	-10.00
	MIP-3	ROAQGWKFRG/a	1603.8	ROAQGWKFRGAWGK	1789.94	ROAQGWKFRGAWGKR	1946.04	2.00
	MIP-4	EPTWNLKGMW/a	1374.6	EPTWNLKGMWGK	1560.76	EPTWNLKGMWGKR	1716.86	-10.00
	MIP-5	DQWQKLHGGW/a	1253.6	DQWQKLHGGWGK	1439.72	DQWQKLHGGWGKR	1595.82	-7.64
	MS	TDVDHFLRF/a	1247.65	TDVDHFLRFGR	1433.75	TDVDHFLRFGRK	1589.86	-8.42
Neuropeptide F	MS (2-9)	DVDHFLRF/a	1146.61	DVDHFLRFGR	1332.71	DVDHFLRFGRK	1488.81	-
	NPF	KNDVNTMADAYKFLDDITYGDRARVFa	3484.71	KNDVNTMADAYKFLDDITYGDRARVFEK	3670.81	KNDVNTMADAYKFLDDITYGDRARVFEKR	3826.91	-7.86
Neuropeptide-like precursor 1	MTYa	YIGSLARAGGLMTY/a	1471.77	YIGSLARAGGLMTYGK	1657.87	YIGSLARAGGLMTYGKR	1813.97	-7.29
	IPNa	NVGTLRDFQLPIPI/a	1653.9	NVGTLRDFQLPIPIGK	1840.01	NVGTLRDFQLPIPIGKR	1996.11	-8.25
Pigment-dispersing factor	VQO	NLGALKSSPVHG/VQO	1534.83	NLGALKSSPVHG/VQOK	1662.93	NLGALKSSPVHG/VQOKK	1819.03	-7.87
	APK	SVAALAAAGLLNAPK	1423.83	SVAALAAAGLLNAPKR	1579.93	SVAALAAAGLLNAPKRK	1736.03	-7.80
	PDF	NSELINLSLLSPKMNDAa	1972.02	NSELINLSLLSPKMNDAKG	2158.12	NSELINLSLLSPKMNDAKGR	2314.22	-10.00

(Continues)

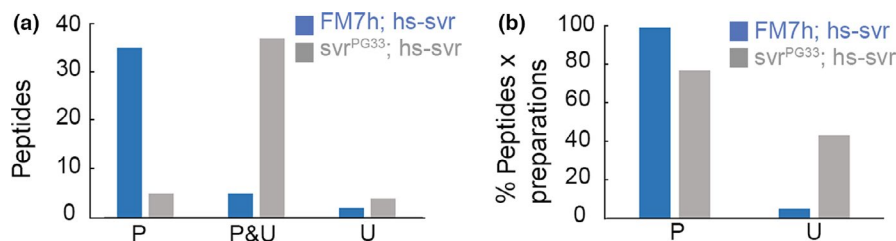


FIGURE 2 Summary of the processed and unprocessed neuropeptide forms identified by direct peptide profiling. (a) Number of different peptides found only either in a fully processed (left) or fully unprocessed C-terminally extend form (right), or in both forms (middle) throughout all analysed samples. (b) Same data as in (a), but now presented as fractions per individual preparations. The data show that unprocessed peptides are more abundant in *svr*^{PG33}; *hs-svr* mutants than in *FM7h*; *hs-svr* control flies, for which unprocessed peptides occurred only for a few specific peptides (see text and Figure S1). In contrast, processed peptides are more abundant in *FM7h*; *hs-svr* control flies than in *svr*^{PG33}; *hs-svr* mutants. [Colour figure can be viewed at wileyonlinelibrary.com]

peaks over all preparations, fully processed forms were found, while peptides carrying a C-terminal basic amino acid extension occurred in only 5% of the peptide peaks over all preparations (Figures 2 and S2).

In *svr*^{PG33}; *hs-svr* experimental flies, 37 neuropeptides were detectable by mass match in both processed bioactive and C-terminal extended form. To test the validity of the mass matching, we sequenced masses matching APK-R, AstA-4, CAPA-PK⁽²⁻¹⁵⁾-GKR, CAPA-PVK-1, corazonin-GKR, FMRFa-2-GR, FMRFa-3-GR, FMRFa-4-GR, FMRFa-6, FMRFa-6-GR, HUG-PK-GKR, IPNa-GKR, myosuppressin-GRR, SIFa and sNPF-1⁽⁴⁻¹¹⁾-GR by MS/MS fragmentation and consistently confirmed their supposed identity (Table 1). Five neuropeptides (Ast-C, CCHa-2, FMRFa-8, MIP-3 and MIP-5) were exclusively found in their processed bioactive form. Four neuropeptides (CCAP, kinin, MIP-2 and PDF) were exclusively found in their unprocessed C-terminally extended form (Figure S2). 76.8% of the mass peaks corresponded to fully processed forms, and 43.2% matched peptides with C-terminal basic amino acid extension (Figures 2 and S2). The qualitative results obtained by direct peptide profiling indicate that the occurrence of unprocessed C-terminally extended neuropeptides is highly increased across the peptidome in *svr*^{PG33}; *hs-svr* flies, suggesting that dCPD is involved in the processing of most if not all neuropeptides.

To obtain a more quantitative measure, we next used nanoLC-ESI-MS/MS and analysed relative differences in the detection levels of processed and unprocessed peptides in brain extracts of *svr*^{PG33}; *hs-svr* mutant flies and *FM7h*;

hs-svr controls. Representative data are shown for allatostatin A and FMRF-like peptides in Figure 3. For each neuropeptide, we calculated a processing index (PI, see material and methods) as a measure of the relative differences in processed vs. unprocessed peptides between *svr*^{PG33}; *hs-svr* mutant flies and *FM7h*; *hs-svr* controls (Table 1, underlying ratios are shown in Figure S3). A PI = 1 means that the ratio of processed to unprocessed forms of a peptide is unchanged between control and mutant flies, a PI > 1 means that there is more processed peptide in the mutants, while a PI < 1 means there is more unprocessed peptide in the mutant compared with control files. With exception of MIP-3 (PI = 100), the long forms of sNPF-1 (PI = 1.7) and sNPF-2 (PI = 50.6), DTK-3 (PI = 1.0) and DTK-5 (PI = 1.4), all peptides had a PI < 0.1, confirming that dCPD is required for C-terminal trimming and peptide processing. In *FM7h*; *hs-svr* controls, all peptides were exclusively detected in their fully processed form ($R = 100$), with exception for AstA-1 and NPLP1-IPNa. Unprocessed AstA-1 was found in one out of three samples ($R = 12.5$), and unprocessed NPLP1-IPNa occurred in two out of three samples ($R = 12.4$ and 1.9). In *svr*^{PG33}; *hs-svr* mutant flies, most peptides were found in both processed and unprocessed forms, confirming the results from MALDI-TOF peptide profiling. LC-MS also confirmed the MALDI-TOF detection of exclusively unprocessed kinin, MIP-2 and PDF in the mutant (PI = 10⁻¹⁰). Also corazonin, MIP-1 and MIP-4 were exclusively detectable in their unprocessed form. Further, MIP-3 but not MIP-5 and FMRFa-8 was found

FIGURE 3 Examples of the LC-MS peptide analysis for two peptide families, allatostatin A and FMRFa-like peptides. Identified peptides were aligned to the prepropeptide sequence. For both peptide families, fully processed and bioactive peptides are C-terminally amidated (red box); both spacer peptides and bioactive peptides were found. In *FM7h*; *hs-svr* control flies, only fully processed amidated bioactive peptides or mostly processed but not yet amidated (still carrying a C-terminal glycine amidation signal) are visible, with exception for AstA-1 (VERYAFGLa) which seems to have a weak C-terminal PC cleavage site. In *svr*^{PG33}; *hs-svr* mutant flies, additional C-terminally extended peptides become detectable which still comprise the C-terminal PC cleavage sequence (KR, RR, R). Interestingly, a mutated carboxypeptidase D (dCPD) leads sometimes to a skip of PC cleavage between some directly neighboured bioactive peptide sequences in both peptide families. Perhaps, intermediate dCPD action is required between two consecutive PC cleavage events in these cases. [Colour figure can be viewed at wileyonlinelibrary.com]

Allatostatin A

1 MNSLHAHLLLLAVCCVGYIAS**SPVIGDQQRSGDSDADVLLAADEMADNGGDNIDK**VERYAF**GLGRRAY**MYTNGGPGMKR**LPVYNFGLGKR**SRPYS**FGLG**

FM7h;hs-svr run 1

101 KRSDYDYDQDNEIDYR**VPPANYLAAE**RAVRPGRQNK**R**T**TRPQPFNFGLGRR**

1 MNSLHAHLLLLAVCCVGYIAS**SPVIGDQQRSGDSDADVLLAADEMADNGGDNIDK**VERYAF**GLGRRAYMYTNGGPGMKR**LPVYN**FGLGKR**SRPYS**FGLG**

svr^{PG33};hs-svr run 2

101 **KR**SDYDYDQDNEIDYR**VPPANYLAAE**RAVRPGRQNK**R**T**TRPQPFNFGLGRR**

FMRFa-like peptides

1 MGIALMFLLLALYQMSAIHSEIIDTPNYAGNSLQDADSEVSPSQDNDLVDALLGNDQTERAELEFRHPISVIGIDYSKNAVVLHFQKHGRKPRYKYDPEL

101 EA**KRR**SVQDN**FMHF**GKRQAEQLPPEGSYAGSDELEGM**AKRAAMD**RYGRDPKQ**DFMR**FGRDPKQDFMR**FGRDPKQDFMR**FGRDPKQDFMR

FM7h;hs-svr run 1

201 FGR**TPAEDFMR**FGRTPAEDFMR**FGRSDNFMR**FGR**SPHEELRSPKQDFMR**FGR**PDNFMR**FGR**SAPQDFVRS**GMDSN**FIR**FGKSLKPAAPESKPVKSNQGN

1 MGIALMFLLLALYQMSAIHSEIIDTPNYAGNSLQDADSEVSPSQDNDLVDALLGNDQTERAELEFRHPISVIGIDYSKNAVVLHFQKHGRKPRYKYDPEL

101 EA**KRR**SVQDN**FMHF**GKRQAEQLPPEGSYAGSDELEGM**AKRAAMD**RYGRDPKQ**DFMR**FGRDPKQDFMR**FGRDPKQDFMR**FGRDPKQDFMR

svr^{PG33};hs-svr run 3

201 FGR**TPAEDFMR**FGRTPAEDFMR**FGRSDNFMR**FGR**SPHEELRSPKQDFMR**FGR**PDNFMR**FGR**SAPQDFVRS**GMDSN**FIR**FGKSLKPAAPESKPVKSNQGN

a amidation (-0.98)
o oxidation (M) (+15.99)
p pyro-Glu from Q (17.03)

in exclusively processed form in the mutant. Like MIP-3, also the long forms of sNPF-1 (sNPF-1₁₋₁₁) and sNPF-2 (sNPF-2₁₋₁₉) were only detectable in the mutant, but occurred with a smaller peak area also in the unprocessed forms. This explains the positive PIs for these peptides (Table 1). The presence of only processed MIP-3 in mutant flies is difficult to account for. sNPF-1₁₋₁₁ and sNPF-2₁₋₁₀ have been found with lower signal intensity in previous neuropeptidomic studies (Baggerman et al., 2002, 2005; Nässel, Enell, Santos, Wegener, & Johard, 2008; Predel et al., 2004; Wegener et al., 2006; Yew et al., 2009). The existence of the long form sNPF-2₁₋₁₉ is shown here for the first time, although this peptide was predicted from the *Drosophila* genome (Vanden Broeck, 2001). Possibly, the proper intrapeptide processing at monobasic arginine sites to yield the sequence-identical short sNPF forms (sNPF₄₋₁₁, sNPF-2₁₂₋₁₉) requires dCPD trimming. Taken together, the results of direct mass spectrometric MALDI-TOF profiling

and LC-ESI-MS indicate that dCPD is a key enzyme in neuropeptide processing.

3.3 | *svr* is broadly expressed throughout the larval and adult CNS

The peptidome-wide impairment of neuropeptide processing in *svr*^{PG33}, *hs-svr* mutants suggested that dCPD is broadly expressed in peptidergic neurons throughout the CNS. To test this, we made use of the intragenic Gal4 sequence contained within the inserted enhancer-trap element PGawB of *svr*^{PG33} (Bourbon et al., 2002) and drove the expression of either a membrane-bound or nuclear form of UAS-GFP. In both the larval and adult CNS, a large number of neurons innervating basically all neuropiles expressed *svr*^{PG33}-Gal4-driven GFP (Figure 4a). This is in line with the idea that many *Drosophila* neurons express peptide co-transmitters (Nässel, 2018).

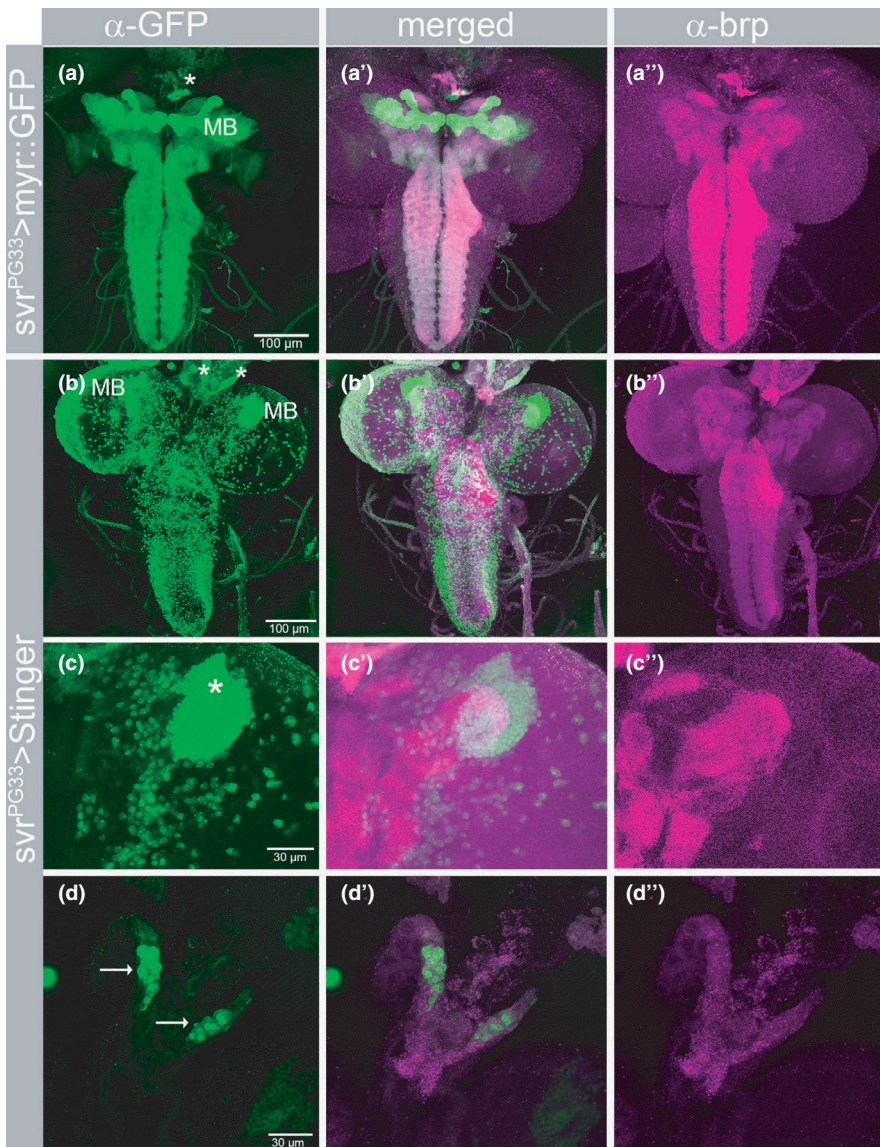


FIGURE 4 *svr* expression pattern based on the intragenic PG33 insert. The Gal4 sequence contained within the PG33 GawB insert was used to drive either a membrane-bound (myr::GFP, a) or nuclear (Stinger) form of GFP (b–d) in the larval central nervous system. Staining with mAb nc82 against the synaptic protein bruchpilot was used to mark neuropil areas (a''–d''). Maximum projections of confocal stacks. (a) The whole neuropil is uniformly innervated by *svr*^{PG33}-expressing neurons, only the densely packed mushroom bodies (MB) stick out. In the attached ring gland, the endocrine cells producing adipokinetic hormone are also strongly labelled (asterisk). (b) The nuclear staining shows that many but by far not all neurons express *svr*^{PG33}. Again, the Kenyon cells forming the mushroom bodies (MB) as well as the adipokinetic hormone (AKH) cells (asterisks) are conspicuous. (c) Close-up of the MB shown in (b) shows the densely packed Kenyon cell somata (asterisk) in the dorsal protocerebrum. (d) Close-up of the AKH cells in (b), located in the corpora cardiaca portion of the ring gland. [Colour figure can be viewed at wileyonlinelibrary.com]

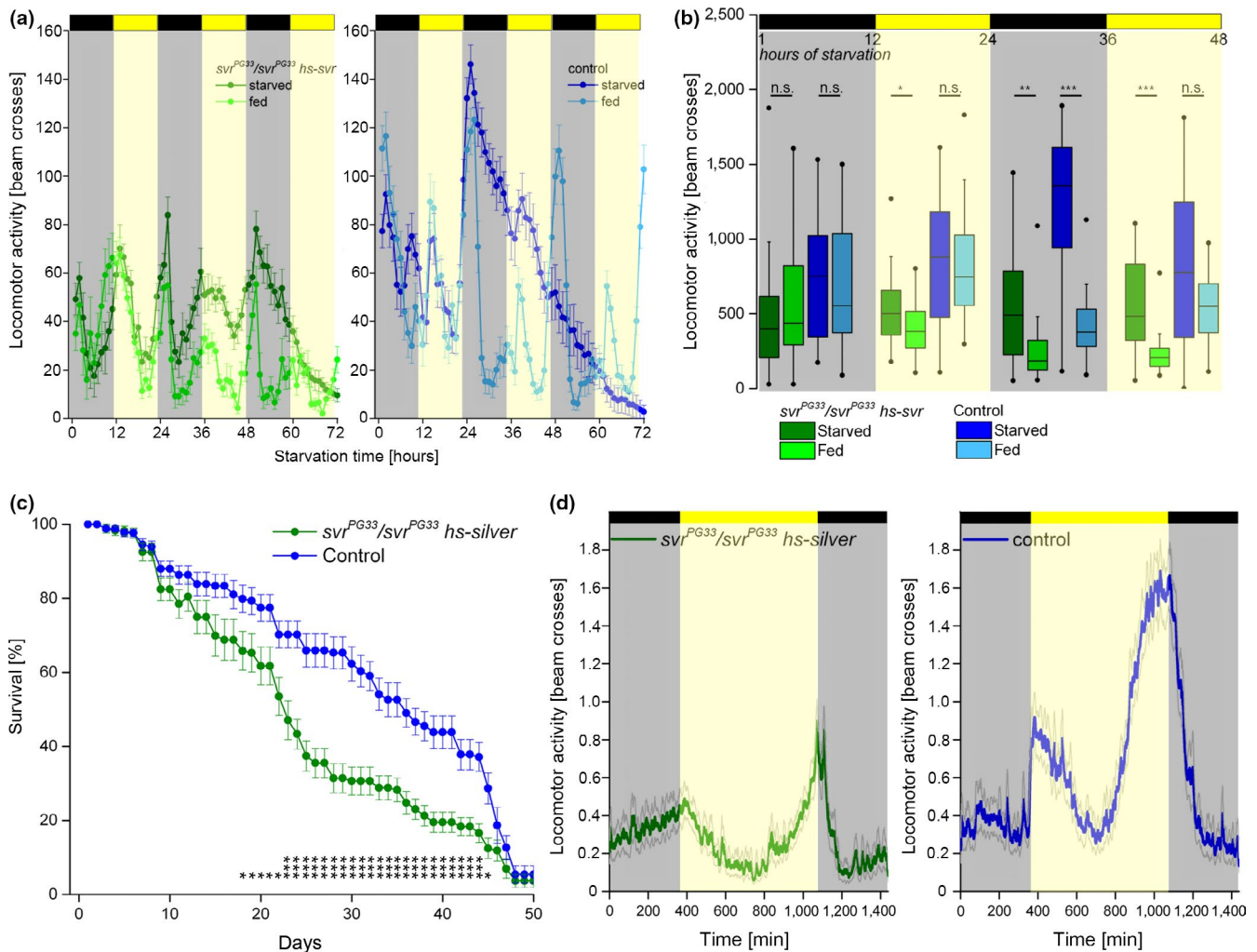


FIGURE 5 Carboxypeptidase D is required for starvation-induced hyperactivity and affects survival rate and locomotor activity. (a) *svr^{PG33}/svr^{PG33} hs-svr* mutant flies showed an early onset of starvation-induced hyperactivity (~20 hr) during the first day without food. In contrast, control flies started starvation-induced hyperactivity later, during the second night after ~30 hr of starvation. (b) Statistic comparison of averaged locomotor activity for the first two nights and days after starvation onset. $n = 23\text{--}29$. (c) Survival is significantly lower between day 18 and day 45 in *svr^{PG33}/svr^{PG33} hs-silver* mutant flies compared with control flies. (d) Total locomotor activity in *svr^{PG33}/svr^{PG33} hs-silver* mutant flies is significantly reduced ($p = 5 \times 10^{-14}$) compared with control flies, especially during morning and evening activity bouts. Yet, daily rhythmicity remains unaffected. $n = 53\text{--}61$. Significance level $*p < .05$, $**p < .01$, $***p < .001$. [Colour figure can be viewed at wileyonlinelibrary.com]

Due to the broad expression, it was impossible to identify specific arborisation patterns except for the tightly packed Kenyon cells with their parallel projections in the mushroom bodies (Figure 4a–c). These neurons express sNPF (Johard et al., 2008; Nässel et al., 2008). As sNPF processing was impaired in *svr^{PG33}/svr^{PG33} hs-svr* flies (Table 1, Figure S2), dCPD likely plays a role in peptide processing in these higher order integration centres. Outside of the CNS, the conspicuous endocrine AKH cells in the glandular part of the corpora cardiaca and the proximal part of the larval ring gland were strongly labelled (Figure 4a,d). This is compatible with the finding that genetic manipulations of dCPD levels in these cells significantly affect AKH processing (Sidyelyeva et al., 2010).

3.4 | dCPD is required for starvation-induced hyperactivity

The expression pattern of *svr^{PG33}* suggested that dCPD is expressed in AKH-producing endocrine cells of the corpora cardiaca. AKH has metabolic functions and is required for starvation-induced hyperactivity (Lee & Park, 2004; Yu et al., 2016). To address the functional requirement of dCPD in AKH processing, we tested whether starvation-induced hyperactivity is affected in *svr^{PG33}/svr^{PG33} hs-svr* mutant flies (Figure 5a,b). At ZT 12 (lights off), flies were placed into monitor tubes containing either only agarose (starvation condition) or agarose and sucrose (control condition). All genotypes showed significant starvation-induced hyperactivity during the experiment on agarose (Figure 5a). *svr^{PG33}/svr^{PG33} hs-svr* mutant flies

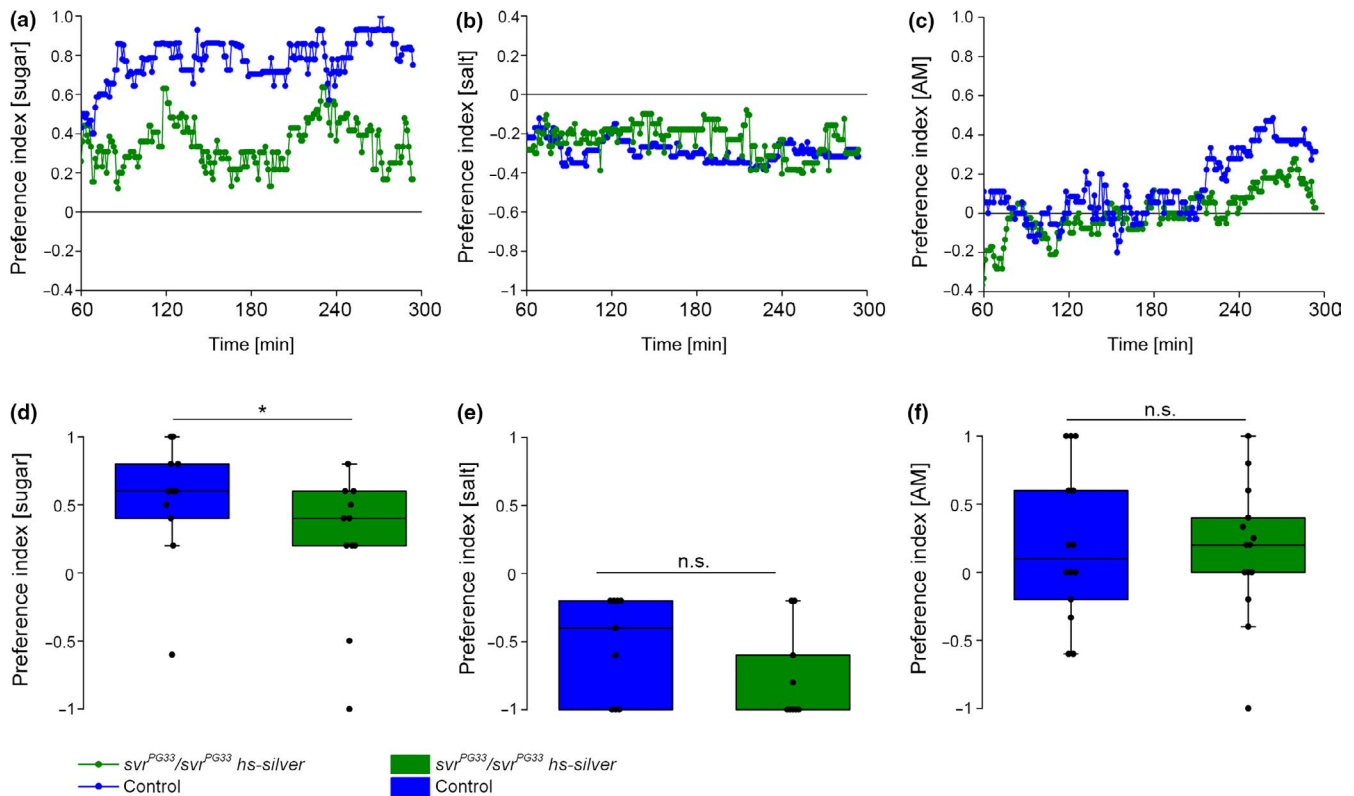


FIGURE 6 Carboxypeptidase D affects appetitive, but not aversive taste or odour responses. (a,d) *svr^{PG33}, hs-svr* mutant larvae showed a reduced preference behaviour for fructose compared with control larvae. (b,e) *svr^{PG33}, hs-svr* mutant larvae avoided high salt concentration similar to control larvae over the course of time. (c,e) Odour response to amyloacetate was indistinguishable between *svr^{PG33}, hs-svr* mutant larvae and control larvae. $n = 30\text{--}42$. Significance level $*p < .05$. n.s., not significant. [Colour figure can be viewed at wileyonlinelibrary.com]

increased their locomotor activity already during the first day (12–24 hr of starvation), while controls still showed normal day activity. During the following night (24–36 hr of starvation), also control larvae increased their locomotor activity to a significant level (Figure 5b). The maximal levels of activity of *svr^{PG33}, hs-svr* mutant flies were quite stable throughout the 72 hr under starvation, and locomotor activity still showed daily rhythmicity with distinguishable peaks during morning and evening and intermediate siesta phase from 24 to 60 hr. In contrast, locomotor activity of control flies peaked during the second night after 24–36 hr of starvation, and then steadily declined until all flies had died at 72 hr without any sign of a siesta phase. Thus, *svr^{PG33}, hs-svr* mutant flies showed reduced hyperactivity compared with controls, in which starvation-induced hyperactivity completely overruled the daily activity pattern. This phenotype is compatible with the assumption of a hypomorphic alteration of AKH processing.

3.5 | Loss of dCPD affects life span and general activity levels

We next assessed the general health state of *svr^{PG33}, hs-svr* mutant flies by analysing their locomotor activity level and life span. Both *svr^{PG33}, hs-svr* mutant and control flies showed

a maximum life span of around 50 days under ad libitum feeding conditions at 25°C. Yet, *svr^{PG33}, hs-svr* mutant flies showed a significantly higher mortality rate between day 18 and day 45 compared with control flies (Figure 5c). Next, we analysed locomotor activity and rhythmicity. Control flies displayed the characteristic bimodal activity pattern with increased morning and evening activity and a siesta phase during mid-day. *svr^{PG33}, hs-svr* mutant flies showed the same rhythmicity, yet an overall reduced activity pattern, with dampened morning and evening activity bouts (Figure 5d).

3.6 | dCPD is required for appetitive but not aversive gustatory preference

Neuropeptides act both as signalling and as modulatory substances within chemosensory input pathways in *Drosophila* (Hückesfeld, Peters, & Pankratz, 2016; Root, Ko, Jafari, & Wang, 2011; Shankar et al., 2015; Winther, Acebes, & Ferrús, 2006). We therefore used larval preference assays (Selcho, Pauls, Huser, Stocker, & Thum, 2014) to test whether dCPD-mediated peptide processing plays a role in gustatory or olfactory signalling. First, we tested the preference for fructose, a sugar that provides nutritional value and sweetness (Rohwedder et al., 2012). *svr^{PG33}, hs-svr* mutant

TABLE 2 Taxonomic distribution of identified putative insect CPD/CPE sequences

Taxon	CPD	CPE
Hexapoda		
Collembola	✓	✓
Diplura	– ^a	✓
Hemimetabolous insects		
Ephemeroptera	– ^a	✓
Odonata	– ^a	✓
Orthoptera	✓	– ^a
Phasmatodea	– ^a	✓
Dictyoptera	✓	✓
Phtiraptera	✓	✓
Hemiptera	✓	✓
Holometabolous insects		
Hymenoptera	✓	–
Coleoptera	✓	✓
Diptera	✓	– ^b
Lepidoptera	✓	✓

^aOnly restricted sequence data analysed.

^bPutative CPE sequences were found for tephritid fly species.

larvae showed approach behaviour for fructose; however, the performance was reduced compared with control larvae in the course of time (Figure 6a) and significantly reduced after 5 min (Figure 6d). To test whether a lack of dCPD generally affects gustatory responses, we challenged larvae with aversive high salt concentrations. As expected, control larvae significantly avoided high salt concentrations. Similarly, *svr*^{PG33}, *hs-svr* mutant larvae showed avoidance behaviour, suggesting that the lack of dCPD affected the larval response specifically to sugar or appetitive substances and not taste responses in general (Figure 6b,e). Next, we tested larvae for their innate olfaction. *svr*^{PG33}, *hs-svr* mutant larvae and control larvae performed indistinguishable over the course of time and approached amylicetate (Figure 6c,f). Our results suggest that hypomorphic dCPD levels do not affect chemosensory sensory processing in general, but rather gustatory responses to sugar.

3.7 | Evidence for an independent loss of CPE but not CPD in holometabolous insects

Carboxypeptidase E, the major neuropeptide processing CP in mammals, has also been found in molluscs (Juvvadi, Fan, Nagle, & Fricker, 1997) and nematodes (Husson et al., 2007; Jacob & Kaplan, 2003), but is absent in *Drosophila*

(Sidyelyeva & Fricker, 2002). To test whether this lack of CPE applies to insects in general, we performed a nonexhaustive insect genome BLAST search based on CPE sequences from mouse and *C. elegans* (EGL-21), and CPD sequences from *Drosophila*. Obtained insect CPE sequences were then used to refine the search. In total, we obtained 310 predicted full CP sequences from insects covering the major insect orders. This analysis certainly does not include all available sequence information for insects, and we did not specifically search for CP sequences within individual genomes. A maximum-likelihood tree clustered CPE and CPD/CPM separately of each other (Figure S4). CPDs are significantly larger than CPEs and CPMs due to their three CP domains. This criterion was used to separate CPDs from CPMs which otherwise show high sequence similarity between their active CP domains. Our BLAST search yields CPD sequences for most insect orders (Table 2), except for diplurans, mayflies (Ephemeroptera), dragonflies (Odonata) and stick insects (Phasmatodea) for which little genomic data are available and CPD sequences are likely to be found in the future. A conservative interpretation of the data is that all insect orders for which abundant genomic data are available possess CPD (Table 2). CPE was found in the basal Entognatha and in the majority of insect orders including most hemimetabolous orders and the holometabolous beetles and derived Lepidoptera (butterflies, moths and allies) (Table 2). Interestingly, putative CPE sequences could not be identified from those large holometabolous orders which contain the majority of insects with sequenced genomes: the Diptera (mosquitoes, flies and allies) and the Hymenoptera (bees, ants, wasps and allies) (Table 2). Thus, CPE seems to be common throughout the insects, but apparently has been independently lost at least two times: in the basal holometabolous Hymenoptera, as well as the derived holometabolous Diptera. A puzzling finding not concurrent with this notion is the presence of a putative CPE sequence in the snowberry fruit fly *Rhagoletis zephyria* but not other species belonging to the *Tephritidae* (true fruit flies, not directly related to the *Drosophilidae* (vinegar flies)). The size and sequence including the first and second block of Zn²⁺ binding residues classifies this predicted CP as CPE. We also found a true CPD gene for *R. zephyria* as well as other tephritid species, speaking against a gene prediction or sequencing error. Further studies are required to confirm and explain the surprising putative presence of CPE in a tephritid.

4 | DISCUSSION

N/E metallo-carboxypeptidases of the M14 family catalyse the second step in prepropeptide processing by removing the C-terminal mono- or dibasic cleavage signal that remains after proprotein convertase cleavage of the propeptide (Fricker, 2013a). Peptidomic studies detected a large and

broad accumulation of C-terminally extended neuropeptides in *Cpe^{fat}/Cpe^{fat}* mice (Che, Biswas, et al., 2005; Che, Yuan, et al., 2005; Che et al., 2001) and *egl-21* mutant *C. elegans* (Husson et al., 2007). This indicated that CPE is the key carboxypeptidase for neuropeptide processing in these phylogenetically very distant animals. It was thus surprising that the genome of the fruit fly *Drosophila* lacks a CPE-encoding gene (Sidyelyeva & Fricker, 2002; Taghert & Veenstra, 2003), the only insect in which neuropeptide processing is studied in more detail (Pauls et al., 2014). Several lines of evidence indicated that dCPD encoded by *svr* has taken over the key function of neuropeptide processing in *Drosophila*. First, the second domain of dCPD has enzymatic properties similar to those of mammalian CPE (Sidyelyeva & Fricker, 2002). While mammals have only one main splice form of CPD mRNA and CPD is absent from mature secretory vesicles that contain CPE (Varlamov, Eng, Novikova, & Fricker, 1999; Varlamov & Fricker, 1998), dCPD mRNA has various splice forms. Of these, the long forms carrying tail-1 likely are located mostly to vesicles outside the perinuclear area when expressed in *Drosophila* and mammalian cell lines (Kalinina, Fontenele-Neto, & Fricker, 2006), mimicking the localisation pattern of mammalian CPE. Next, ectopic expression of *svr* in the endocrine AKH-producing cells reduced the levels of naturally occurring C-terminally extended AKH (Sidyelyeva et al., 2010). Lastly, flies with disrupted *svr* gene are embryonically lethal (Settle et al., 1995; Sidyelyeva et al., 2006) and show deficits in various neuropeptide-regulated behaviours (Sidyelyeva et al., 2006). Direct evidence for an involvement of CPD in neuropeptide processing was, however, lacking so far for any species, including the fruit fly. Hence, a main result of our peptidomic study is the demonstration of the ability of dCPD to efficiently process a broad variety of neuropeptides. This raises the possibility that the failure of mouse CPD to fully rescue a deficiency of CPE (Song & Fricker, 1995) is caused by an incomplete overlap of the CPD and CPE expression patterns in peptidergic neurons rather than by a reduced efficiency of mouse CPD to process neuropeptides.

The early lethality of *svr* mutants (Settle et al., 1995; Sidyelyeva et al., 2006) suggests that dCPD function during development cannot be substituted by dCPM. Our finding that *svr^{PG33}* mutant larvae and pupae required daily heat-shock rescue to develop into adults is in line with the importance of *svr* during development. Yet, once adult, *svr^{PG33}* mutants survived without heat shock even though the mean life span was significantly reduced. Our RT-PCR results suggest that this reduced viability is due to a background expression of the *hs-svr* rescue construct even at lower temperature and not due to a loss of dCPD requirement in adult flies. We had previously observed a similar phenomenon for *amon* (dPC2)-deficient flies rescued by a *hs-amon* construct (Wegener et al., 2011). We hypothesise that the production rate of neuropeptides is significantly lower in adult flies than

in the very fast growing larva or developing pupa, in which the background expression of either *hs-amon* or *hs-svr* may not be sufficient to provide the required increasing supply in neuropeptides during development. Alternatively, adults may better cope with reduced levels of neuropeptides and possible other products of CPD action which presumably are less critical for post-developmental viability, at least under laboratory conditions.

Taken together, our results suggest that dCPD is a key if not the sole CP involved in neuropeptide processing in *Drosophila*.

As a mutation in either *amon* or *svr* is lethal, it is surprising why during evolution *Drosophila* has kept only one gene for a proprotein convertase (dPC2, *amon*; Wegener et al., 2011) and one peptide processing CP (CPD, *svr*, this study), given that most animals have additional genes (PC1/3 and CPE). The fact that CPD and not CPE has been kept could be explained by the potential higher versatility of CPD with its two bioactive domains and membrane-anchored and free isoforms which have unique functions, substrate specificities and specific pH optima (Garcia-Pardo et al., 2017; Sidyelyeva et al., 2010). It is tempting to speculate that dCPD has further functions additional to neuropeptide processing, which cannot be executed by CPE with its single bioactive domain. This is in line with the finding that hypomorphic *svr* mutants have phenotypes in wing morphology (Sidyelyeva et al., 2006) and biogenic amine pools (Wright, 1987). This hypothesis is also supported by our finding that obviously CPE has been independently lost at least twice during insect evolution in Hymenoptera and Diptera, while CPD seems to be present in all insect taxa. Functionally, it will be interesting to see whether other insects have various CPD mRNA splice variants and whether the number of variants correlates with the presence of CPE.

Based on the expression pattern of the *svr^{PG33}* transgene, dCPD is broadly expressed in the CNS and neuroendocrine organs. The expression in the Kenyon cells of the mushroom body, an important brain centre for learning and memory, is in line with impaired long-term memory in a courtship assay (Sidyelyeva et al., 2010) and olfactory memory formation (Lu et al., 2016) found in *svr* hypomorphs. Similarly, knockout of CPE in mice impairs olfactory social learning, object recognition memory and performance in the Morris water maze (Woronowicz et al., 2008). The expression of *svr^{PG33}* in the AKH cells of the corpora cardiaca, as well as its effect on AKH-mediated starvation-induced hyperactivity, indicates a role of dCPD in AKH processing after dPC2 cleavage (Rhea et al., 2010). This is supported by the effect of ectopically expressed dCPD on AKH processing as shown by direct peptide profiling (Sidyelyeva et al., 2010).

Impairment in insulin signalling increases life span (Brogiolo et al., 2001; Tatar et al., 2001), and dCPD has been implicated in insulin processing (Lu et al., 2016). Yet, we found the mean life span of the *svr^{PG33}* hypomorphs is

decreased which suggests a further, unidentified role of dCPD outside of peptide processing or an involvement of other yet unknown neuropeptides in the regulation of life span. These neuropeptides could be identified by cell-specific *svr* knock-out via CRISPR-Cas9 (Xue et al., 2014) or knockdown via RNAi, as the *svr^{PG33}* driver line lends itself as a tool to generally impair peptide signalling in neurons even if these express multiple co-expressed or unknown peptides.

Taken together, our results show that dCPD is a key enzyme for neuropeptide processing in *Drosophila*, and is required for proper peptide-regulated behaviour. The finding that CPE but not CPD has been independently lost in two major insect taxa may point to important further CPD functions beyond neuropeptide processing which cannot be fulfilled by CPE.

ACKNOWLEDGEMENTS

We thank Lloyd Fricker and Galina Sidyelyeva for the generous gift of plasmids and flies, the Bloomington Stock Center for providing fly lines, and the *Drosophila* Genomics Resource Center for the generous gift of *svr* constructs, Henry-Marc Bourbon for detailed information on the *svr^{PG33}* insert, Lloyd Fricker, Vera Terblanche and two unknown reviewers for helpful comments and discussions, and Susanne Klühspies for excellent laboratory support. Funded by intramural support of the University of Würzburg.

CONFLICT OF INTEREST

We declare no conflict of interests.

DATA AVAILABILITY STATEMENT

Dataset: Original data available at Dryad <https://doi.org/10.5061/dryad.82pr5td>.

AUTHOR CONTRIBUTIONS

DP and CW designed the study; YH, JTV, AS, JK and CW performed and analysed the mass spectrometric measurements; YH and CW performed immunostainings; DP and LT performed and analysed the behavioural assays; TS and GG created the *svr-hs* construct; LT and GG performed RT-PCR; CW performed the phylogenomic analysis; and CW and DP wrote the manuscript draft. All authors read and commented on the final manuscript version.

ORCID

Dennis Pauls  <https://orcid.org/0000-0001-8330-8120>

Yasin Hamarat  <https://orcid.org/0000-0002-1343-5068>

Jens T. Vanselow  <https://orcid.org/0000-0001-8900-8209>

Christian Wegener  <https://orcid.org/0000-0003-4481-3567>

REFERENCES

- Audsley, N., Matthews, H. J., Down, R. E., & Weaver, R. J. (2011). Neuropeptides associated with the central nervous system of the cabbage root fly, *Delia radicum* (L.). *Peptides*, 32, 434–440.
- Baggerman, G., Boonen, K., Verleyen, P., De Loof, A., & Schoofs, L. (2005). Peptidomic analysis of the larval *Drosophila melanogaster* central nervous system by two-dimensional capillary liquid chromatography quadrupole time-of-flight mass spectrometry. *Journal of Mass Spectrometry*, 40, 250–260.
- Baggerman, G., Cerstiaens, A., De Loof, A., & Schoofs, L. (2002). Peptidomics of the larval *Drosophila melanogaster* central nervous system. *Journal of Biological Chemistry*, 277, 40368–40374.
- Bourbon, H.-M., Gonzy-Treboul, G., Peronnet, F., Alin, M.-F., Ardourel, C., Benassayag, C., ... Vincent, A. (2002). A P-insertion screen identifying novel X-linked essential genes in *Drosophila*. *Mechanisms of Development*, 110, 71–83.
- Brehme, K. S. (1941). The effect of adult body color mutations upon the larva of *Drosophila melanogaster*. *Proceedings of the National Academy of Sciences of the United States of America*, 27, 254–261.
- Broggiolo, W., Stocker, H., Ikeya, T., Rintelen, F., Fernandez, R., & Hafen, E. (2001). An evolutionarily conserved function of the *Drosophila* insulin receptor and insulin-like peptides in growth control. *Current Biology*, 11, 213–221.
- Che, F.-Y., Biswas, R., & Fricker, L. D. (2005). Relative quantitation of peptides in wild-type and Cpe(fat/fat) mouse pituitary using stable isotopic tags and mass spectrometry. *Journal of Mass Spectrometry*, 40, 227–237.
- Che, F. Y., & Fricker, L. D. (2002). Quantitation of neuropeptides in Cpefat/Cpefat mice using differential isotopic tags and mass spectrometry. *Analytical Chemistry*, 74, 3190–3198.
- Che, F. Y., Yan, L., Li, H., Mzhavia, N., Devi, L. A., & Fricker, L. D. (2001). Identification of peptides from brain and pituitary of Cpe(fat)/Cpe(fat) mice. *Proceedings of the National Academy of Sciences of the United States of America*, 98, 9971–9976.
- Che, F.-Y., Yuan, Q., Kalinina, E., & Fricker, L. D. (2005). Peptidomics of Cpe fat/fat mouse hypothalamus: Effect of food deprivation and exercise on peptide levels. *Journal of Biological Chemistry*, 280, 4451–4461.
- Chintapalli, V. R., Wang, J., & Dow, J. A. T. (2007). Using FlyAtlas to identify better *Drosophila melanogaster* models of human disease. *Nature Genetics*, 39, 715–720.
- Diesner, M., Gallot, A., Binz, H., Gaertner, C., Vitecek, S., Kahnt, J., ... Gadenne, C. (2018). Mating-induced differential peptidomics of neuropeptides and protein hormones in *Agrotis ipsilon* moths. *Journal of Proteome Research*, 17, 1397–1414.
- Feng, Y., Ueda, A., & Wu, C.-F. (2004). A modified minimal hemolymph-like solution, HL3.1, for physiological recordings at the neuromuscular junctions of normal and mutant *Drosophila* larvae. *Journal of Neurogenetics*, 18, 377–402.
- Fricker, L. D. (2005). Neuropeptide-processing enzymes: Applications for drug discovery. *American Association of Pharmaceutical Scientists Journal*, 7, E449–E455.
- Fricker, L. D. (2013a). Carboxypeptidases E and D. In A. J. Kastin (Ed.), *Handbook of biologically active peptides* (2nd ed., pp. 1715–1720). Boston, MA: Academic Press.
- Fricker, L. D. (2013b). Chapter 300 - Carboxypeptidase E. In N. D. Rawlings & G. Salvesen (Eds.), *Handbook of proteolytic enzymes* (3rd ed., pp. 1342–1345). Amsterdam: Academic Press.

- Fricker, L. D., & Snyder, S. H. (1982). Enkephalin convertase: Purification and characterization of a specific enkephalin-synthesizing carboxypeptidase localized to adrenal chromaffin granules. *Proceedings of the National Academy of Sciences of the United States of America*, *79*, 3886–3890.
- Garcia-Pardo, J., Tanco, S., Diaz, L., Dasgupta, S., Fernandez-Recio, J., Lorenzo, J., ... Fricker, L. D. (2017). Substrate specificity of human metallo-carboxypeptidase D: Comparison of the two active carboxypeptidase domains. *PLoS One*, *12*, e0187778.
- Hadžić, T., Park, D., Abruzzi, K. C., Yang, L., Trigg, J. S., Rohs, R., ... Taghert, P. H. (2015). Genome-wide features of neuroendocrine regulation in *Drosophila* by the basic helix-loop-helix transcription factor DIMMED. *Nucleic Acids Research*, *43*, 2199–2215.
- Hückesfeld, S., Peters, M., & Pankratz, M. J. (2016). Central relay of bitter taste to the protocerebrum by peptidergic interneurons in the *Drosophila* brain. *Nature Communications*, *7*, 12796.
- Husson, S. J., Janssen, T., Baggerman, G., Bogert, B., Kahn-Kirby, A. H., Ashrafi, K., & Schoofs, L. (2007). Impaired processing of FLP and NLP peptides in carboxypeptidase E (EGL-21)-deficient *Caenorhabditis elegans* as analyzed by mass spectrometry. *Journal of Neurochemistry*, *102*, 246–260.
- Jacob, T. C., & Kaplan, J. M. (2003). The EGL-21 carboxypeptidase E facilitates acetylcholine release at *Caenorhabditis elegans* neuromuscular junctions. *Journal of Neuroscience*, *23*, 2122–2130.
- Johard, H. A. D., Enell, L. E., Gustafsson, E., Trifilieff, P., Veenstra, J. A., & Nässel, D. R. (2008). Intrinsic neurons of *Drosophila* mushroom bodies express short neuropeptide F: Relations to extrinsic neurons expressing different neurotransmitters. *Journal of Comparative Neurology*, *507*, 1479–1496.
- Jones, D. T., Taylor, W. R., & Thornton, J. M. (1992). The rapid generation of mutation data matrices from protein sequences. *Computer Applications in the Biosciences*, *8*, 275–282.
- Juvvadi, S., Fan, X., Nagle, G. T., & Fricker, L. D. (1997). Characterization of *Aplysia* carboxypeptidase E. *FEBS Letters*, *408*, 195–200.
- Kalinina, E., Fontenele-Neto, J. D., & Fricker, L. D. (2006). *Drosophila* S2 cells produce multiple forms of carboxypeptidase D with different intracellular distributions. *Journal of Cellular Biochemistry*, *99*, 770–783.
- Krause, E. (1999). The dominance of arginine-containing peptides in MALDI-derived tryptic mass fingerprints of proteins. *Analytical Chemistry*, *71*, 4160–4165.
- Kumar, S., Stecher, G., Li, M., Knyaz, C., & Tamura, K. (2018). MEGA X: Molecular evolutionary genetics analysis across computing platforms. *Molecular Biology and Evolution*, *35*, 1547–1549.
- Lee, G., & Park, J. H. (2004). Hemolymph sugar homeostasis and starvation-induced hyperactivity affected by genetic manipulations of the adipokinetic-hormone-encoding gene in *Drosophila melanogaster*. *Genetics*, *167*, 311–323.
- Lindsley, D. L., & Grell, E. H. (1968). *Genetic variations of Drosophila melanogaster*. Oak Ridge, TN: Carnegie Institute of Washington.
- Lu, B., Zhao, Y., Zhao, J., Yao, X., Shuai, Y., Ma, W., & Zhong, Y. (2016). The carboxypeptidase D homolog silver regulates memory formation via insulin pathway in *Drosophila*. *Protein Cell*, *7*, 606–610.
- Nässel, D. R. (2018). Substrates for neuronal cotransmission with neuropeptides and small molecule neurotransmitters in *Drosophila*. *Frontiers in Cellular Neuroscience*, *12*, 83.
- Nässel, D. R., Enell, L. E., Santos, J. G., Wegener, C., & Johard, H. A. D. (2008). A large population of diverse neurons in the *Drosophila* central nervous system expresses short neuropeptide F, suggesting multiple distributed peptide functions. *BMC Neuroscience*, *9*, 90.
- Pauls, D., Chen, J., Reiher, W., Vanselow, J. T., Schlosser, A., Kahnt, J., & Wegener, C. (2014). Peptidomics and processing of regulatory peptides in the fruit fly *Drosophila*. *EuPA Open Proteomics*, *3*, 114–127.
- Predel, R., Wegener, C., Russell, W. K., Tichy, S. E., Russell, D. H., & Nachman, R. J. (2004). Peptidomics of CNS-associated neurohemal systems of adult *Drosophila melanogaster*: A mass spectrometric survey of peptides from individual flies. *Journal of Comparative Neurology*, *474*, 379–392.
- Rappsilber, J., Mann, M., & Ishihama, Y. (2007). Protocol for micro-purification, enrichment, pre-fractionation and storage of peptides for proteomics using StageTips. *Nature Protocols*, *2*, 1896–1906.
- Rayburn, L. Y., Gooding, H. C., Choksi, S. P., Maloney, D., Kidd, A. R., Siekhaus, D. E., & Bender, M. (2003). *amontillado*, the *Drosophila* homolog of the prohormone processing protease PC2, is required during embryogenesis and early larval development. *Genetics*, *163*, 227–237.
- Rayburn, L. Y. M., Rhea, J., Jocoy, S. R., & Bender, M. (2009). The proprotein convertase *amontillado* (*amon*) is required during *Drosophila* pupal development. *Developmental Biology*, *333*, 48–56.
- Reiher, W., Shirras, C., Kahnt, J., Baumeister, S., Isaac, R. E., & Wegener, C. (2011). Peptidomics and peptide hormone processing in the *Drosophila* Midgut. *Journal of Proteome Research*, *10*, 1881–1892.
- Rhea, J. M., Wegener, C., & Bender, M. (2010). The proprotein convertase encoded by *amontillado* (*amon*) is required in *Drosophila* corpora cardiaca endocrine cells producing the glucose regulatory hormone AKH. *PLoS Genetics*, *6*, e1000967.
- Risse, B., Thomas, S., Otto, N., Löpmeier, T., Valkov, D., Jiang, X., & Klämbt, C. (2013). FIM, a novel FTIR-based imaging method for high throughput locomotion analysis. *PLoS One*, *8*, e53963.
- Rohwedder, A., Pfitzenmaier, J. E., Ramsperger, N., Apostolopoulou, A. A., Widmann, A., & Thum, A. S. (2012). Nutritional value-dependent and nutritional value-independent effects on *Drosophila melanogaster* larval behavior. *Chemical Senses*, *37*, 711–721.
- Root, C. M., Ko, K. I., Jafari, A., & Wang, J. W. (2011). Presynaptic facilitation by neuropeptide signaling mediates odor-driven food search. *Cell*, *145*, 133–144.
- Schachtner, J., Wegener, C., Neupert, S., & Predel, R. (2010). Direct peptide profiling of brain tissue by MALDI-TOF mass spectrometry. *Methods in Molecular Biology*, *615*, 129–135.
- Schindelin, J., Arganda-Carreras, I., Frise, E., Kaynig, V., Longair, M., Pietzsch, T., ... Cardona, A. (2012). Fiji: An open-source platform for biological-image analysis. *Nature Methods*, *9*, 676–682.
- Seidah, N. G., & Prat, A. (2012). The biology and therapeutic targeting of the proprotein convertases. *Nature Reviews Drug Discovery*, *11*, 367–383.
- Selcho, M., Pauls, D., Huser, A., Stocker, R. F., & Thum, A. S. (2014). Characterization of the octopaminergic and tyraminerbic neurons in the central brain of *Drosophila* larvae. *Journal of Comparative Neurology*, *522*, 3485–3500.
- Settle, S. H. Jr, Green, M. M., & Burtis, K. C. (1995). The silver gene of *Drosophila melanogaster* encodes multiple carboxypeptidases similar to mammalian prohormone-processing enzymes. *Proceedings of*

- the National Academy of Sciences of the United States of America*, 92, 9470–9474.
- Shankar, S., Chua, J. Y., Tan, K. J., Calvert, M. E., Weng, R., Ng, W. C., ... Yew, J. Y. (2015). The neuropeptide tachykinin is essential for pheromone detection in a gustatory neural circuit. *eLife*, 4, e06914.
- Sidyelyeva, G., Baker, N. E., & Fricker, L. D. (2006). Characterization of the molecular basis of the *Drosophila* mutations in carboxypeptidase D. Effect on enzyme activity and expression. *Journal of Biological Chemistry*, 281, 13844–13852.
- Sidyelyeva, G., & Fricker, L. D. (2002). Characterization of *Drosophila* carboxypeptidase D. *Journal of Biological Chemistry*, 277, 49613–49620.
- Sidyelyeva, G., Wegener, C., Schoenfeld, B. P., Bell, A. J., Baker, N. E., McBride, S. M. J., & Fricker, L. D. (2010). Individual carboxypeptidase D domains have both redundant and unique functions in *Drosophila* development and behavior. *Cellular and Molecular Life Sciences*, 67, 2991–3004.
- Siekhaus, D. E., & Fuller, R. S. (1999). A role for *amontillado*, the *Drosophila* homolog of the neuropeptide precursor processing protease PC2, in triggering hatching behavior. *Journal of Neuroscience*, 19, 6942–6954.
- Song, L., & Fricker, L. D. (1995). Purification and characterization of carboxypeptidase D, a novel carboxypeptidase E-like enzyme, from bovine pituitary. *Journal of Biological Chemistry*, 270, 25007–25013.
- Steller, H., & Pirrotta, V. (1985). Expression of the *Drosophila* white gene under the control of the *hsp70* heat shock promoter. *EMBO Journal*, 4, 3765–3772.
- Taghert, P. H., & Veenstra, J. A. (2003). *Drosophila* neuropeptide signaling. *Advances in Genetics*, 49, 1–65.
- Tatar, M., Kopelman, A., Epstein, D., Tu, M. P., Yin, C. M., & Garofalo, R. S. (2001). A mutant *Drosophila* insulin receptor homolog that extends life-span and impairs neuroendocrine function. *Science*, 292, 107–110.
- Taylor, N. A., Van de Ven, W. J., & Creemers, J. W. (2003). Curbing activation: Proprotein convertases in homeostasis and pathology. *FASEB Journal*, 17, 1215–1227.
- Thummel, C. S., & Pirrotta, V. (1991). Technical notes: New pCaSperR P-element vectors. *Drosophila Information Newsletter*, 71, 150.
- Vanden Broeck, J. (2001). Neuropeptides and their precursors in the fruitfly, *Drosophila melanogaster*. *Peptides*, 22, 241–254.
- Varlamov, O., Eng, F. J., Novikova, E. G., & Fricker, L. D. (1999). Localization of metalloproteinase D in AtT-20 cells. Potential role in prohormone processing. *Journal of Biological Chemistry*, 274, 14759–14767.
- Varlamov, O., & Fricker, L. D. (1998). Intracellular trafficking of metalloproteinase D in AtT-20 cells: Localization to the trans-Golgi network and recycling from the cell surface. *Journal of Cell Science*, 111, 877–885.
- Wegener, C., Herbert, H., Kahnt, J., Bender, M., & Rhea, J. M. (2011). Deficiency of prohormone convertase dPC2 (AMONTILLADO) results in impaired production of bioactive neuropeptide hormones in *Drosophila*. *Journal of Neurochemistry*, 118, 581–595.
- Wegener, C., Neupert, S., & Predel, R. (2010). Direct MALDI-TOF mass spectrometric peptide profiling of neuroendocrine tissue of *Drosophila*. *Methods in Molecular Biology*, 615, 117–127.
- Wegener, C., Reinl, T., Jansch, L., & Predel, R. (2006). Direct mass spectrometric peptide profiling and fragmentation of larval peptide hormone release sites in *Drosophila melanogaster* reveals tagma-specific peptide expression and differential processing. *Journal of Neurochemistry*, 96, 1362–1374.
- Winther, A. M. E., Acebes, A., & Ferrús, A. (2006). Tachykinin-related peptides modulate odor perception and locomotor activity in *Drosophila*. *Molecular and Cellular Neurosciences*, 31, 399–406.
- Woronowicz, A., Koshimizu, H., Chang, S.-Y., Cawley, N. X., Hill, J. M., Rodriguiz, R. M., ... Loh, Y. P. (2008). Absence of carboxypeptidase E leads to adult hippocampal neuronal degeneration and memory deficits. *Hippocampus*, 18, 1051–1063.
- Wright, T. R. F. (1987). The genetics of biogenic amine metabolism, sclerotization, and melanization in *Drosophila melanogaster*. In J. G. Scandalios, & E. W. Caspari (Eds.), *Advances in genetics, molecular genetics of development* (pp. 127–222). London: Academic Press.
- Xue, Z., Wu, M., Wen, K., Ren, M., Long, L., Zhang, X., & Gao, G. (2014). CRISPR/Cas9 mediates efficient conditional mutagenesis in *Drosophila*. *G3 Bethesda*, 4, 2167–2173.
- Yew, J. Y., Wang, Y., Barteneva, N., Dikler, S., Kutz-Naber, K. K., Li, L., & Kravitz, E. A. (2009). Analysis of neuropeptide expression and localization in adult *Drosophila melanogaster* central nervous system by affinity cell-capture mass spectrometry. *Journal of Proteome Research*, 8, 1271–1284.
- Yu, Y., Huang, R., Ye, J., Zhang, V., Wu, C., Cheng, G., ... Wang, L. (2016). Regulation of starvation-induced hyperactivity by insulin and glucagon signaling in adult *Drosophila*. *eLife*, 5, e15693.
- Zhang, X., & Skidgel, R. A. (2013). Chapter 304 – Carboxypeptidase M. In N. D. Rawlings & G. Salvesen (Eds.), *Handbook of proteolytic enzymes* (3rd ed., pp. 1357–1366). Amsterdam: Academic Press.
- Zhang, J., Xin, L., Shan, B., Chen, W., Xie, M., Yuen, D., ... Ma, B. (2012). PEAKS DB: De Novo sequencing assisted database search for sensitive and accurate peptide identification. *Molecular Cell Proteomics*, 11, M111.010587.
- Zhou, A., Webb, G., Zhu, X., & Steiner, D. F. (1999). Proteolytic processing in the secretory pathway. *Journal of Biological Chemistry*, 274, 20745–20748.

SUPPORTING INFORMATION

Additional supporting information may be found online in the Supporting Information section at the end of the article.

How to cite this article: Pauls D, Hamarat Y, Trufasu L, et al. *Drosophila* carboxypeptidase D (SILVER) is a key enzyme in neuropeptide processing required to maintain locomotor activity levels and survival rate. *Eur J Neurosci*. 2019;50:3502–3519. <https://doi.org/10.1111/ejn.14516>